Beyond Diagonal RIS Design for Parameter Estimation With and Without Eavesdropping

Özlem Tuğfe Demir, *Member, IEEE*, and Sinan Gezici, *Fellow, IEEE*

***Abstract*—In this letter, we study the transmission of a complex-valued parameter vector from a transmitter to an intended receiver in the presence or absence of an eavesdropper. Direct links are blocked, and communication is enabled via a beyond-diagonal reconfigurable intelligent surface (BD-RIS). Extending prior work on diagonal RIS, we incorporate BD-RIS and quantify its impact on estimation performance at the intended receiver, measured by the trace of the Fisher information matrix (FIM), equivalently, the average Fisher information, while constraining the eavesdropper's estimation capability. We propose optimization algorithms for the BD-RIS response and demonstrate their effectiveness. Numerical results show that BD-RIS offers significant gains over conventional RIS. To the best of our knowledge, this is the first study to address secure parameter estimation under BD-RIS architectures with both closed-form and efficient algorithmic solutions.**

***Index Terms*—BD-RIS, Fisher information, parameter estimation, RIS, Cramér-Rao lower bound.**

I. Introduction

EAVESDROPPING stands as a significant security threat in wireless networks, primarily due to the inherently broadcast nature of the wireless medium [1], [2]. Physical layer security (PLS) is a promising approach to ensure confidentiality, which leverages the inherent randomness of wireless channels. The primary objective of PLS-based approaches is to ensure secure communications with the intended receivers in the presence of eavesdroppers by exploiting the unique characteristics of wireless channels [2], [3].

Over the past decade, reconfigurable intelligent surfaces (RISs) have emerged as a key wireless technology for shaping the propagation environment to enhance critical performance metrics. RIS has also been extensively explored in the context of PLS [2], [4]. One of the recent studies has shown that optimized RIS phase profiles can enhance secure parameter estimation by maximizing the trace of the Fisher information matrix (FIM)–also known as the average Fisher information–at the legitimate receiver, while simultaneously limiting the average Fisher information gained by a potential eavesdropper [2].

Conventional RIS architectures employ single-connected elements with independent phase shifts, modeled by a diagonal reflection matrix where each diagonal entry modifies the impinging signal [5]. Recent advances have introduced beyond-diagonal RIS (BD-RIS) architectures, where passive interconnections between elements enable non-diagonal reflection matrices. Shen et al. [6] classify these as fully- or group-connected designs, offering greater flexibility and potential power gains under certain channel conditions [6], [7], [8]. Furthermore, other novel non-diagonal architectures have also been proposed as lower-complexity alternatives to the group-connected design, while offering improved performance [9], [10]. BD-RIS has also recently been integrated into emerging wireless systems such as cell-free massive MIMO with simultaneous wireless information and power transfer, demonstrating its effectiveness in enhancing both spectral efficiency and harvested energy [11].

Unlike conventional diagonal RIS configurations with unit-modulus entries, BD-RIS allows for arbitrary unitary response matrices in the ideal hardware case, with or without symmetry constraints—corresponding to reciprocal or non-reciprocal circuit designs, respectively. However, when the effect of scattering in the radio environment on the mutual coupling between BD-RIS elements is considered, the BD-RIS response matrix becomes subject to stricter constraints compared to the ideal case [12], [13]. The authors of [13] demonstrated the first reflective BD-RIS prototype, showing that reconfigurable inter-element connections offer benefits, though performance gains are strongly influenced by hardware constraints.

While [2] has investigated parameter estimation with conventional RIS, the role of BD-RIS in this setting has not been explored. In this letter, we close this gap by initiating the study of parameter estimation under BD-RIS-assisted transmission, tackling several previously unaddressed problems involving both reciprocal and non-reciprocal surface designs, with and without eavesdropping threats. Our key novelty lies in the formulation of new optimization problems specific to BD-RIS architectures and the development of corresponding closed-form or semi-closed-form solutions. These designs offer gains in estimation accuracy for the legitimate user while mitigating information leakage to a potential eavesdropper.

II. System Model

We adopt the system model proposed in [2], with the key difference that we consider assistance from a BD-RIS instead of a conventional diagonal RIS. A deterministic, k-dimensional complex-valued parameter vector, denoted by $\boldsymbol{\theta} = [\theta_1, \ldots, \theta_k]^T$, is transmitted from Alice (the transmitter) to Bob (the intended receiver). We analyze two distinct scenarios: (i) presence of an eavesdropper (Eve), and (ii) absence of an eavesdropper. The vector $\boldsymbol{\theta}$ is assumed to be unknown to both Bob and Eve. We assume that the direct links between Alice and both Bob and Eve are blocked, and

Received 29 July 2025; revised 10 September 2025; accepted 26 September 2025. Date of publication 30 September 2025; date of current version 12 December 2025. The associate editor coordinating the review of this article and approving it for publication was Y. Mao. *(Corresponding author: Özlem Tuğfe Demir.)*

The authors are with the Department of Electrical and Electronics Engineering, Bilkent University, 06800 Ankara, Türkiye (e-mail: ozlemtugfedemir@bilkent.edu.tr; gezici@ee.bilkent.edu.tr).

Digital Object Identifier 10.1109/LWC.2025.3616123

2162-2345 © 2025 IEEE. All rights reserved, including rights for text and data mining, and training of artificial intelligence and similar technologies. Personal use is permitted, but republication/redistribution requires IEEE permission. See https://www.ieee.org/publications/rights/index.html for more information.
Authorized licensed use limited to: ULAKBIM UASL - Bilkent University. Downloaded on December 11,2025 at 10:40:55 UTC from IEEE Xplore. Restrictions apply.

Alice can reach Bob and Eve through the cascaded channels facilitated by the BD-RIS. In this setting, measurements at Bob and Eve are obtained according to the following linear models [2]:

$$\mathbf{y}_b = (\mathbf{H}_{rb}\boldsymbol{\Omega}\mathbf{H}_{ar})\mathbf{P}\boldsymbol{\theta} + \boldsymbol{\eta}_b \tag{1}$$
$$\mathbf{y}_e = (\mathbf{H}_{re}\boldsymbol{\Omega}\mathbf{H}_{ar})\mathbf{P}\boldsymbol{\theta} + \boldsymbol{\eta}_e \tag{2}$$

where $\mathbf{y}_b \in \mathbb{C}^{n_b}$ and $\mathbf{y}_e \in \mathbb{C}^{n_e}$ represent the received measurement vectors at Bob and Eve, respectively. The matrices $\mathbf{H}_{ar} \in \mathbb{C}^{r\times k}$, $\mathbf{H}_{rb} \in \mathbb{C}^{n_b\times r}$, and $\mathbf{H}_{re} \in \mathbb{C}^{n_e\times r}$ denote the channels corresponding to the Alice–RIS, RIS–Bob, and RIS–Eve links, respectively. The integers k, n_b, n_e, and r denote the dimensionality of the parameter vector, the number of antenna elements at Bob, the number of antenna elements at Eve, and the number of RIS elements, respectively. The noise vectors $\boldsymbol{\eta}_b \in \mathbb{C}^{n_b}$ and $\boldsymbol{\eta}_e \in \mathbb{C}^{n_e}$ are modeled as circularly symmetric complex Gaussian with distributions $\boldsymbol{\eta}_b \sim \mathcal{CN}(\mathbf{0}, \boldsymbol{\Sigma}_b)$ and $\boldsymbol{\eta}_e \sim \mathcal{CN}(\mathbf{0}, \boldsymbol{\Sigma}_e)$, where $\boldsymbol{\Sigma}_b$ and $\boldsymbol{\Sigma}_e$ are positive definite covariance matrices. The power allocation matrix is given by $\mathbf{P} = \mathrm{diag}\{\sqrt{p_1}, \sqrt{p_2}, \ldots, \sqrt{p_k}\}$ and is assumed to be fixed. $\boldsymbol{\Omega}$ is the $r \times r$ BD-RIS response matrix.

As in [2], the trace of the FIM, which indicates the overall usefulness of a measurement for vector parameter estimation [14], is considered as the estimation performance metric due to its tractable and intuitive form, which can be calculated for Bob and Eve as [2, eq. (14)]

$$\mathrm{tr}(\mathbf{I}(\mathbf{y}_b;\boldsymbol{\theta})) = \mathrm{tr}\Big((\mathbf{H}_{rb}\boldsymbol{\Omega}\mathbf{H}_{ar}\mathbf{P})^H\boldsymbol{\Sigma}_b^{-1}(\mathbf{H}_{rb}\boldsymbol{\Omega}\mathbf{H}_{ar}\mathbf{P})\Big) \tag{3}$$
$$\mathrm{tr}(\mathbf{I}(\mathbf{y}_e;\boldsymbol{\theta})) = \mathrm{tr}\Big((\mathbf{H}_{re}\boldsymbol{\Omega}\mathbf{H}_{ar}\mathbf{P})^H\boldsymbol{\Sigma}_e^{-1}(\mathbf{H}_{re}\boldsymbol{\Omega}\mathbf{H}_{ar}\mathbf{P})\Big). \tag{4}$$

III. BD-RIS Design Without Eavesdropping

To begin with, we omit the eavesdropper and only consider the intended user, Bob. The trace of the FIM for Bob can be written from (3) as

$$\mathrm{tr}(\mathbf{I}(\mathbf{y}_b;\boldsymbol{\theta})) = \mathrm{tr}\Big(\mathbf{P}^H\mathbf{H}_{ar}^H\boldsymbol{\Omega}^H\mathbf{H}_{rb}^H\boldsymbol{\Sigma}_b^{-1}\mathbf{H}_{rb}\boldsymbol{\Omega}\mathbf{H}_{ar}\mathbf{P}\Big) \tag{5}$$
$$= \mathrm{tr}\Big(\mathbf{H}^H\boldsymbol{\Omega}^H\boldsymbol{E}_b\boldsymbol{\Omega}\mathbf{H}\Big) \tag{6}$$

with $\boldsymbol{E}_b \triangleq \mathbf{H}_{rb}^H\boldsymbol{\Sigma}_b^{-1}\mathbf{H}_{rb} \in \mathbb{C}^{r\times r}$ and $\mathbf{H} \triangleq \mathbf{H}_{ar}\mathbf{P} \in \mathbb{C}^{r\times k}$. We first focus on the following optimization problem:

$$\max_{\boldsymbol{\Omega}} \quad \mathrm{tr}\Big(\mathbf{H}^H\boldsymbol{\Omega}^H\boldsymbol{E}_b\boldsymbol{\Omega}\mathbf{H}\Big) \tag{7a}$$
$$\text{subject to} \quad \boldsymbol{\Omega}^H\boldsymbol{\Omega} = \mathbf{I}_r \tag{7b}$$

where $\mathbf{I}_r$ is the $r \times r$ identity matrix and $\boldsymbol{\Omega}$ is the $r \times r$ BD-RIS response matrix, specified as a complex unitary matrix in the constraint. Here, we consider the most general form of a fully connected BD-RIS, where the reciprocity constraint (symmetric $\boldsymbol{\Omega}$) is relaxed.[1] In fact, non-reciprocal circuit networks can practically be realized, and solving this problem yields the ultimate limit on the average Fisher information—analogous to capacity limits in communication systems [15].

We can express the optimization problem in (7) as

$$\max_{\boldsymbol{\Omega}} \quad \mathrm{tr}\Big(\boldsymbol{\Omega}^H\boldsymbol{E}_b\boldsymbol{\Omega}\boldsymbol{M}\Big) \tag{8a}$$
$$\text{subject to} \quad \boldsymbol{\Omega}^H\boldsymbol{\Omega} = \mathbf{I}_r \tag{8b}$$

where $\boldsymbol{M} \triangleq \mathbf{H}\mathbf{H}^H \in \mathbb{C}^{r\times r}$.

The solution of (8) is specified in the following lemma.

Lemma: The optimal BD-RIS response matrix for the problem (8) is given as $\boldsymbol{\Omega} = \boldsymbol{V}_E\boldsymbol{V}_M^H$, where $\boldsymbol{V}_E$ and $\boldsymbol{V}_M$ are the unitary matrices with the columns as the eigenvectors of $\boldsymbol{E}_b$ and $\boldsymbol{M}$, respectively. The eigenvectors are arranged to correspond to the eigenvalues, which are sorted in descending order.

Proof: We use $\boldsymbol{E}_b = \boldsymbol{V}_E\boldsymbol{\Delta}_E\boldsymbol{V}_E^H$ and $\boldsymbol{M} = \boldsymbol{V}_M\boldsymbol{\Delta}_M\boldsymbol{V}_M^H$ for denoting the eigenvalue decompositions of $\boldsymbol{E}_b$ and $\boldsymbol{M}$, respectively. The diagonal matrices $\boldsymbol{\Delta}_E$ and $\boldsymbol{\Delta}_M$ have the eigenvalues arranged in descending order along their diagonals. Since $\boldsymbol{\Omega}^H\boldsymbol{E}_b\boldsymbol{\Omega}$ and $\boldsymbol{M}$ are positive semi-definite matrices and the eigenvalues of $\boldsymbol{\Omega}^H\boldsymbol{E}_b\boldsymbol{\Omega}$ and $\boldsymbol{E}_b$ are the same (due to unitary $\boldsymbol{\Omega}$), we have from Von Neumann's trace inequality

$$\mathrm{tr}\Big(\boldsymbol{\Omega}^H\boldsymbol{E}_b\boldsymbol{\Omega}\boldsymbol{M}\Big) \le \sum_{i=1}^{r}\delta_{E,i}\delta_{M,i}, \tag{9}$$

where $\delta_{E,1} \ge \delta_{E,2} \ge \cdots \ge \delta_{E,r}$ and $\delta_{M,1} \ge \delta_{M,2} \ge \cdots \ge \delta_{M,r}$ are the sorted eigenvalues in $\boldsymbol{\Delta}$ and $\boldsymbol{\Sigma}$, respectively. We then observe that inserting $\boldsymbol{\Omega} = \boldsymbol{V}_E\boldsymbol{V}_M^H$ results in this upper bound. Hence, it is an optimal configuration. ■

Now, we consider the average Fisher information maximization problem for a reciprocal BD-RIS by adding the symmetry constraint as

$$\max_{\boldsymbol{\Omega}} \quad \mathrm{tr}\Big(\boldsymbol{\Omega}^H\boldsymbol{E}_b\boldsymbol{\Omega}\boldsymbol{M}\Big) \tag{10a}$$
$$\text{subject to} \quad \boldsymbol{\Omega}^H\boldsymbol{\Omega} = \mathbf{I}_r \text{ and } \boldsymbol{\Omega} = \boldsymbol{\Omega}^T. \tag{10b}$$

This problem can be solved using manifold optimization techniques as in [16], where the overall steps of the main alternating optimization (AO) algorithm are outlined in Algorithm 1. The initialization point is taken as $\boldsymbol{\Omega}_0 = \boldsymbol{U}\boldsymbol{U}^T$, where $\boldsymbol{U}$ is the unitary matrix obtained from the Takagi singular value decomposition of $\boldsymbol{V}_E\boldsymbol{V}_M^H + \boldsymbol{V}_M^*\boldsymbol{V}_E^T$ as

$$\boldsymbol{V}_E\boldsymbol{V}_M^H + \boldsymbol{V}_M^*\boldsymbol{V}_E^T = \boldsymbol{U}\boldsymbol{\Sigma}\boldsymbol{U}^T. \tag{11}$$

As derived in [8, Th. 1], $\boldsymbol{\Omega}_0 = \boldsymbol{U}\boldsymbol{U}^T$ is the closest entry of the set determined by $\boldsymbol{\Omega}^H\boldsymbol{\Omega} = \mathbf{I}_r$ and $\boldsymbol{\Omega} = \boldsymbol{\Omega}^T$ to $\boldsymbol{V}_E\boldsymbol{V}_M^H$ which is the optimal configuration when there is no reciprocity constraint. The computational complexity of Algorithm 1 is dominated by the Takagi singular value decomposition [17] in the initialization and the eigenvalue decomposition in computing $e^{\mu\boldsymbol{S}_{\text{skew}}}$, which is in the order of $\mathcal{O}((I+1)r^3)$, where I is the iteration number.

IV. Secure BD-RIS Design in the Presence of Eavesdropping

In this section, there also exists an eavesdropper, Eve, in the environment. The average Fisher information at Eve can be expressed via (4) as

$$\mathrm{tr}(\mathbf{I}(\mathbf{y}_e;\boldsymbol{\theta})) = \mathrm{tr}\Big(\mathbf{P}^H\mathbf{H}_{ar}^H\boldsymbol{\Omega}^H\mathbf{H}_{re}^H\boldsymbol{\Sigma}_e^{-1}\mathbf{H}_{re}\boldsymbol{\Omega}\mathbf{H}_{ar}\mathbf{P}\Big)$$
$$= \mathrm{tr}\Big(\mathbf{H}^H\boldsymbol{\Omega}^H\boldsymbol{E}_e\boldsymbol{\Omega}\mathbf{H}\Big) = \mathrm{tr}\Big(\boldsymbol{\Omega}^H\boldsymbol{E}_e\boldsymbol{\Omega}\boldsymbol{M}\Big) \tag{12}$$

where $\boldsymbol{E}_e \triangleq \mathbf{H}_{re}^H\boldsymbol{\Sigma}_e^{-1}\mathbf{H}_{re}$. Then, the optimization problem in the presence of eavesdropping for non-reciprocal BD-RIS (the

[1]This letter adopts an ideal unitary BD-RIS response matrix to enable tractable optimization and theoretical analysis. However, such assumptions may oversimplify the physical behavior of practical RIS circuits. For a detailed physics-compliant modeling approach, see [12].

Authorized licensed use limited to: ULAKBIM UASL - Bilkent University. Downloaded on December 11,2025 at 10:40:55 UTC from IEEE Xplore. Restrictions apply.

Algorithm 1 AO Algorithm for Solving (10)

1: **Initialization:** Select $\boldsymbol{\Omega}_0 = \boldsymbol{U}\boldsymbol{U}^T$, where $\boldsymbol{U}$ is obtained from (11). Set the iteration counter to zero, i.e., $i = 0$. Convergence threshold: ϵ. Learning step size $\mu > 0$
2: **while** Improvement in the cost function larger than ϵ **do**
3: Compute the gradient of the cost function with respect to $\boldsymbol{U}^*$ as $\boldsymbol{Z} = \boldsymbol{E}_b\boldsymbol{U}_i\boldsymbol{U}_i^T\boldsymbol{M}\boldsymbol{U}_i^*$
4: Compute $\boldsymbol{U}_i e^{\mu \boldsymbol{S}_{\text{skew}}}$, where $e^{\mu \boldsymbol{S}_{\text{skew}}}$ is the matrix exponential and $\boldsymbol{S}_{\text{skew}} = \frac{\boldsymbol{U}_i^H\boldsymbol{Z} - \boldsymbol{Z}^H\boldsymbol{U}_i}{2}$.
5: If there is a cost improvement, increase μ, update $\boldsymbol{U}_{i+1}$ as $\boldsymbol{U}_i e^{\mu \boldsymbol{S}_{\text{skew}}}$ and cost function. Otherwise, decrease μ and do not change $\boldsymbol{U}_i$ and the cost.
6: $i \leftarrow i + 1$
7: **end while**
8: **Output:** $\boldsymbol{\Omega} = \boldsymbol{U}_i\boldsymbol{U}_i^T$

most general form) can be written as

$$\max_{\boldsymbol{\Omega}} \ \operatorname{tr}\left(\boldsymbol{\Omega}^H\boldsymbol{E}_b\boldsymbol{\Omega}\boldsymbol{M}\right) \tag{13a}$$
$$\text{subject to} \ \ \boldsymbol{\Omega}^H\boldsymbol{\Omega} = \mathbf{I}_r \tag{13b}$$
$$\operatorname{tr}\left(\boldsymbol{\Omega}^H\boldsymbol{E}_e\boldsymbol{\Omega}\boldsymbol{M}\right) \le \epsilon \tag{13c}$$

where we limit the average Fisher information at Eve by $\epsilon > 0$.

We first re-express the problem in (13) as

$$\max_{\boldsymbol{\Omega},\boldsymbol{\Psi}} \ \Re\left(\operatorname{tr}\left(\boldsymbol{\Omega}^H\boldsymbol{E}_b\boldsymbol{\Psi}\boldsymbol{M}\right)\right) \tag{14a}$$
$$\text{subject to} \ \ \boldsymbol{\Omega}^H\boldsymbol{\Omega} = \mathbf{I}_r, \quad \boldsymbol{\Psi} = \boldsymbol{\Omega} \tag{14b}$$
$$\operatorname{tr}\left(\boldsymbol{\Psi}^H\boldsymbol{E}_e\boldsymbol{\Psi}\boldsymbol{M}\right) \le \epsilon. \tag{14c}$$

Then, we adopt the penalty dual decomposition (PDD) method [7], [18] to solve the problem in (14), since it has been shown to be effective for optimization problems of a similar type [7]. To this end, the augmented Lagrangian function is obtained as

$$\mathcal{L}(\boldsymbol{\Omega},\boldsymbol{\Psi},\boldsymbol{\Lambda}) = -\Re\left(\operatorname{tr}\left(\boldsymbol{\Omega}^H\boldsymbol{E}_b\boldsymbol{\Psi}\boldsymbol{M}\right)\right) + \frac{1}{2\rho}\|\boldsymbol{\Omega}-\boldsymbol{\Psi}\|_F^2 + \Re\left(\operatorname{tr}\left(\boldsymbol{\Lambda}^H(\boldsymbol{\Omega}-\boldsymbol{\Psi})\right)\right) \tag{15}$$

where $\boldsymbol{\Lambda}$ is the Lagrangian dual variable associated with the constraint $\boldsymbol{\Psi} = \boldsymbol{\Omega}$ and ρ^{-1} is the penalty coefficient. The steps outlined in the following subsections are repeated until convergence as described in [7, Algorithm 1] with the major difference in the inner layer updates as outlined below. We empirically observe consistent convergence in all our experiments.

A. Update Ω of PDD Inner Layer Iteration

The augmented Lagrangian minimization problem in terms of $\boldsymbol{\Omega}$ can be written as

$$\min_{\boldsymbol{\Omega}} \ \ \|\boldsymbol{\Omega} - (\boldsymbol{\Psi} + \rho\boldsymbol{E}_b\boldsymbol{\Psi}\boldsymbol{M} - \rho\boldsymbol{\Lambda})\|_F^2 \tag{16a}$$
$$\text{subject to} \ \ \boldsymbol{\Omega}^H\boldsymbol{\Omega} = \mathbf{I}_r \tag{16b}$$

which can analytically be solved using [7, Lemma 1].

B. Update $\boldsymbol{\Psi}$ of PDD Inner Layer Iteration

The augmented Lagrangian minimization problem in terms of $\boldsymbol{\Psi}$ can be written as

$$\min_{\boldsymbol{\Psi}} \ \ \left\|\boldsymbol{\Psi} - \left(\boldsymbol{\Omega} + \rho\boldsymbol{E}_b^H\boldsymbol{\Omega}\boldsymbol{M}^H + \rho\boldsymbol{\Lambda}\right)\right\|_F^2 \tag{17a}$$
$$\text{subject to} \ \ \operatorname{tr}\left(\boldsymbol{\Psi}^H\boldsymbol{E}_e\boldsymbol{\Psi}\boldsymbol{M}\right) \le \epsilon \tag{17b}$$

which can be cast as a quadratically-constrained quadratic programming form by vectorizing the matrices. Using the vec Kronecker identity in [19], we can express the problem as

$$\min_{\mathbf{x}} \ \ \|\mathbf{x} - \mathbf{b}\|^2 \tag{18a}$$
$$\text{subject to} \ \ \mathbf{x}^H\mathbf{A}\mathbf{x} \le \epsilon \tag{18b}$$

where $\mathbf{b} = \operatorname{vec}(\boldsymbol{\Omega} + \rho\boldsymbol{E}_b^H\boldsymbol{\Omega}\boldsymbol{M}^H + \rho\boldsymbol{\Lambda})$, $\mathbf{x} = \operatorname{vec}(\boldsymbol{\Psi})$, and $\mathbf{A} = \boldsymbol{M}^T \otimes \boldsymbol{E}_e$.

To solve the above problem in semi-closed form, we first express the eigenvalue decomposition of $\mathbf{A}$ as $\mathbf{A} = \sum_{i=1}^{r^2}\lambda_i\mathbf{u}_i\mathbf{u}_i^H$, where $\lambda_i \ge 0$ is the ith eigenvalue with the corresponding unit-norm eigenvector $\mathbf{u}_i \in \mathbb{C}^{r^2}$. We then express the optimization variable as $\mathbf{x} = \sum_{i=1}^{r^2}\alpha_i e^{j\phi_i}\mathbf{u}_i$, where $\alpha_i > 0$ and the phase-shift ϕ_i are the newly defined optimization variables. The problem can then be written as

$$\min_{\{\alpha_i,\phi_i\}} \ \ \left\|\sum_{i=1}^{r^2}\alpha_i e^{j\phi_i}\mathbf{u}_i - \mathbf{b}\right\|^2 \tag{19a}$$
$$\text{subject to} \ \ \sum_{i=1}^{r^2}\lambda_i\alpha_i^2 \le \epsilon \tag{19b}$$

where the optimal phase-shifts are obtained as $\phi_i = \angle\mathbf{u}_i^H\mathbf{b}$, which leads to the optimization problem in terms of $\{\alpha_i\}$ as

$$\min_{\{\alpha_i\}} \ \ \sum_{i=1}^{r^2}\alpha_i^2 - \sum_{i=1}^{r^2}2\alpha_i\left|\mathbf{u}_i^H\mathbf{b}\right| \tag{20a}$$
$$\text{subject to} \ \ \sum_{i=1}^{r^2}\lambda_i\alpha_i^2 \le \epsilon. \tag{20b}$$

The Lagrangian function for (20) is given by

$$\mathcal{L}(\{\alpha_i\},\mu) = \sum_{i=1}^{r^2}\alpha_i^2 - \sum_{i=1}^{r^2}2\alpha_i\left|\mathbf{u}_i^H\mathbf{b}\right| + \mu\left(\sum_{i=1}^{r^2}\lambda_i\alpha_i^2 - \epsilon\right) \tag{21}$$

where $\mu \ge 0$ is the Lagrange multiplier. Then, the Karush-Kuhn-Tucker (KKT) conditions are stated as follows:

$$\frac{\partial\mathcal{L}}{\partial\alpha_i} = 2\alpha_i - 2\left|\mathbf{u}_i^H\mathbf{b}\right| + 2\mu\lambda_i\alpha_i = 0, \tag{22}$$

which yields

$$\alpha_i = \frac{|\mathbf{u}_i^H\mathbf{b}|}{1+\mu\lambda_i}, \quad \sum_{i=1}^{r^2}\lambda_i\alpha_i^2 \le \epsilon, \tag{23}$$
$$\mu \ge 0, \quad \mu\left(\sum_{i=1}^{r^2}\lambda_i\alpha_i^2 - \epsilon\right) = 0. \tag{24}$$

To determine the optimal value of μ, we first set $\mu = 0$, then $\alpha_i = |\mathbf{u}_i^H\mathbf{b}|$, and we check if the constraint holds. If $\sum_{i=1}^{r^2}\lambda_i|\mathbf{u}_i^H\mathbf{b}|^2 \le \epsilon$, then this is the optimal solution. Otherwise, we solve for μ such that

$$\sum_{i=1}^{r^2}\lambda_i\left(\frac{|\mathbf{u}_i^H\mathbf{b}|}{1+\mu\lambda_i}\right)^2 = \epsilon. \tag{25}$$

This equation in μ can be solved via a bisection search.

Authorized licensed use limited to: ULAKBIM UASL - Bilkent University. Downloaded on December 11,2025 at 10:40:55 UTC from IEEE Xplore. Restrictions apply.

C. Update of PDD Outer Layer Iteration

For updating the PDD outer layer iteration, the procedure in [7, eqs. (31)-(32)] is applied.

When solving the optimization problem for the reciprocal BD-RIS, an additional symmetry constraint arises, which affects only the update of $\mathbf{\Omega}$ in the inner iteration of the PDD algorithm. This update is implemented by solving

$$\min_{\mathbf{\Omega}} \quad \|\mathbf{\Omega} - (\mathbf{\Psi} + \rho \boldsymbol{E}_b \mathbf{\Psi} \boldsymbol{M} - \rho \mathbf{\Lambda})\|_F^2 \qquad (26a)$$

$$\text{subject to} \quad \mathbf{\Omega}^H \mathbf{\Omega} = \mathbf{I}_r \text{ and } \mathbf{\Omega} = \mathbf{\Omega}^T \qquad (26b)$$

which can analytically be solved using [8, Th. 1].

Remark 1: The transmitter can learn the channel related to Eve, $\mathbf{H}_{re}$, by estimating her location (e.g., via a camera or performing sensing as in integrated sensing and communication systems, e.g., [20]), and then by using theoretical or empirical channel models to determine the channel matrix between the BD-RIS and Eve (considering the fact that there exists line-of-sight between them). The uncertainty in estimating $\mathbf{H}_{re}$ can be modeled via a statistical approach, and the average value of the trace of the FIM at Eve can be considered as the secrecy constraint, which can be derived as $\mathrm{tr}(\mathbf{\Omega}^H \overline{\boldsymbol{E}}_e \mathbf{\Omega} \boldsymbol{M})$ with $\overline{\boldsymbol{E}}_e \triangleq \mathbb{E}[\mathbf{H}_{re}^H \mathbf{\Sigma}_e^{-1} \mathbf{H}_{re}]$. Since this is in the same form as (13c), all the results can still be applied.

The computational complexity of the PDD algorithm is dominated by the eigenvalue decomposition of the $r^2 \times r^2$ matrix $\mathbf{A}$, which leads to $\mathcal{O}(r^6)$. This complexity exceeds that of the conventional RIS-based design in [2], which is $\mathcal{O}(r^{4.5} \log(1/\epsilon))$, where ϵ denotes the solution accuracy parameter.

V. Numerical Results

In this section, we quantify the performance improvements achieved via BD-RIS over the conventional diagonal RIS by leveraging the proposed theoretical and algorithmic solutions to the considered optimization problems. Following the methodology in [2], the real and imaginary parts of the channel matrices are generated as independent and identically distributed (i.i.d.) random variables uniformly drawn from the interval $[-0.1, 0.1]$, based on a single realization in MATLAB. The covariance matrices of the additive noise vectors at Bob and Eve are set to 10^{-5} times the identity matrix. The number of antennas at both Bob and Eve is set as $n_b = n_e = 2k$, where k is the number of parameters. The power allocation matrix is set to $\sqrt{30/k}$ times identity corresponding to equal power allocation.

For diagonal RIS assisted design in the absence of eavesdropping, the semidefinite programming (SDP) problem without the constraint related to Eve, as formulated in [2], is solved, and Gaussian randomization is applied to extract a rank-one solution. In the presence of eavesdropping, it is observed that small values of ϵ—corresponding to a stringent estimation quality threshold for Eve—often result in infeasible problems when the RIS response matrix is constrained to have unit-modulus diagonal entries. To address this issue, we relax the constraint to allow diagonal entries with magnitudes less than or equal to one as in [2, Section V.B] and solve the corresponding positive semidefinite programming problem. After solving that problem, Gaussian randomization is performed,

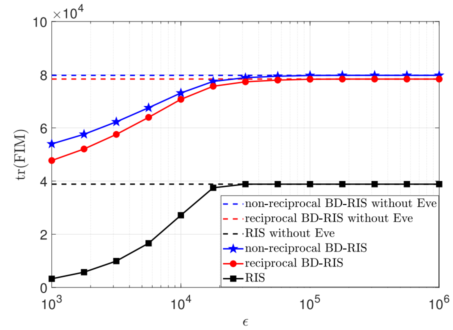

Fig. 1. Trace of FIM at Bob achieved by non-reciprocal BD-RIS, reciprocal BD-RIS, and conventional RIS in both the presence and absence of eavesdropping for $r = 36$ and $k = 10$.

and any diagonal entry of the RIS response matrix exceeding unit magnitude is clipped to have unit modulus.

In Fig. 1, we set the number of BD-RIS and RIS elements to $r = 36$, and the number of parameters to be estimated to $k = 10$. We compare three configurations: i) non-reciprocal BD-RIS without symmetry constraints on the response matrix; ii) reciprocal BD-RIS with symmetry constraints; and iii) conventional diagonal RIS. The *x*-axis of the figure represents the average Fisher information limit of Eve, denoted by ϵ. The dashed lines indicate the average Fisher information at Bob in the absence of eavesdropping; since they do not depend on ϵ, they represent the ultimate achievable average Fisher information limit. We note that Algorithm 1 improves the initial solution by 53% in terms of trace of the FIM. The solid curves correspond to scenarios with eavesdropping. As ϵ increases, the average information at Bob approaches the corresponding ultimate limit. As expected, the highest information is obtained with the non-reciprocal BD-RIS, as it represents the most general form of BD-RIS. Imposing the reciprocity constraint leads to a slight reduction in average Fisher information, although the degradation is negligible. In contrast, when employing a conventional diagonal RIS, the Fisher information is significantly reduced, especially when Eve's information constraint is stringent (i.e., small ϵ). These results demonstrate that BD-RIS notably enhances the estimation performance at Bob even under tight information leakage constraints to Eve.

In Fig. 2, we plot the Cramér–Rao bound (CRB), defined as the trace of the inverse FIM using the same setup as in Fig. 1. Since the maximum likelihood estimator (MLE) achieves the CRB for linear models with additive Gaussian noise as in (1) and (2), the *y*-axis of Fig. 2 also corresponds to the mean-squared error (MSE) of the MLE at Bob. As the figure illustrates, the BD-RIS significantly reduces the CRB, indicating improved estimation accuracy in terms of MSE. This improvement is particularly pronounced when the information leakage to Eve is tightly constrained (i.e., when ϵ is small). Moreover, BD-RIS enables the system to maintain a favorable CRB even under stringent leakage constraints, demonstrating its robustness in secure parameter estimation.

In Figs. 3 and 4, we repeat the previous experiments with a larger BD-RIS and RIS size ($r = 64$) and an increased number of parameters ($k = 15$). As shown in the figures, the estimation quality is further enhanced when using BD-RIS

Authorized licensed use limited to: ULAKBIM UASL - Bilkent University. Downloaded on December 11,2025 at 10:40:55 UTC from IEEE Xplore. Restrictions apply.

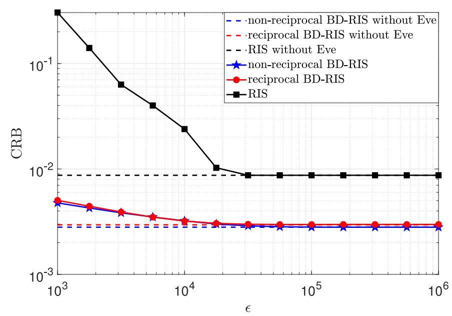

Fig. 2. CRB (equivalently, MSE of the MLE) at Bob achieved by non-reciprocal BD-RIS, reciprocal BD-RIS, and conventional RIS in both the presence and absence of eavesdropping for $r = 36$ and $k = 10$.

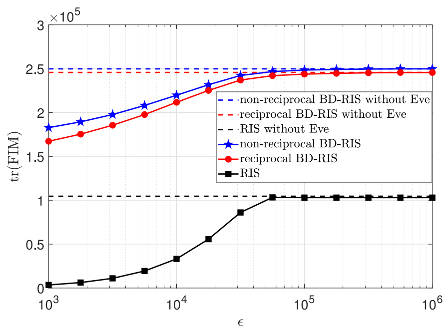

Fig. 3. Trace of FIM at Bob achieved by non-reciprocal BD-RIS, reciprocal BD-RIS, and conventional RIS in both the presence and absence of eavesdropping for $r = 64$ and $k = 15$.

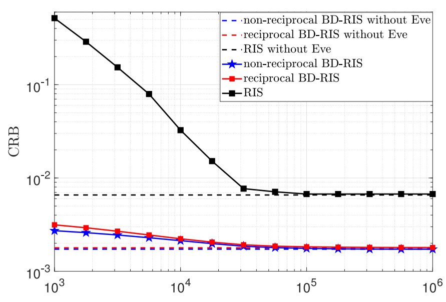

Fig. 4. CRB (equivalently, MSE of the MLE) at Bob achieved by non-reciprocal BD-RIS, reciprocal BD-RIS, and conventional RIS in both the presence and absence of eavesdropping for $r = 64$ and $k = 15$.

compared to conventional RIS. The performance gap between the non-reciprocal and reciprocal BD-RIS designs remains negligible, indicating that the more easily implementable reciprocal circuit networks offer a practical and effective alternative for BD-RIS deployment. Once again, we observe that BD-RIS enables robust and secure estimation even in the presence of eavesdropping.

VI. Conclusion

In this letter, we proposed a BD-RIS architecture for secure parameter estimation in wireless systems, considering both the presence and absence of an eavesdropper. By formulating and solving optimization problems for the BD-RIS response matrix under different constraints—non-reciprocal, reciprocal, and diagonal—we quantified the fundamental performance limits using the trace of the FIM. Our results demonstrate that BD-RISs significantly outperform conventional diagonal RISs, particularly in scenarios with stringent eavesdropping constraints. Furthermore, the performance degradation due to the reciprocity constraint is shown to be negligible, making reciprocal BD-RIS a practical and effective alternative that eliminates the need for non-reciprocal circuit networks. These findings highlight the strong potential of BD-RIS in enhancing secure and accurate wireless parameter estimation.

References

[1] Q. He et al., "Proactive anti-eavesdropping with trap deployment in wireless networks," *IEEE Trans. Dependable Secure Comput.*, vol. 20, no. 1, pp. 637–649, Jan./Feb. 2023.

[2] E. M. Abadi et al., "Joint RIS phase profile design and power allocation for parameter estimation in presence of eavesdropping," *IEEE Trans. Veh. Technol.*, vol. 73, no. 12, pp. 19186–19202, Dec. 2024.

[3] A. Yener and S. Ulukus, "Wireless physical-layer security: Lessons learned from information theory," *Proc. IEEE*, vol. 103, no. 10, pp. 1814–1825, Oct. 2015.

[4] M. H. Khoshafa et al., "RIS-assisted physical layer security in emerging RF and optical wireless communication systems: A comprehensive survey," *IEEE Commun. Surveys Tuts.*, vol. 27, no. 4, pp. 2156–2203, 4th Quart., 2025.

[5] H. Li et al., "Reconfigurable intelligent surfaces 2.0: Beyond diagonal phase shift matrices," *IEEE Wireless Commun. Mag.*, vol. 62, no. 3, pp. 102–108, Mar. 2024.

[6] S. Shen et al., "Modeling and architecture design of reconfigurable intelligent surfaces using scattering parameter network analysis," *IEEE Trans. Wireless Commun.*, vol. 21, no. 2, pp. 1229–1243, Feb. 2022.

[7] Y. Zhou et al., "Optimizing power consumption, energy efficiency, and sum-rate using beyond diagonal RIS—A unified approach," *IEEE Trans. Wireless Commun.*, vol. 23, no. 7, pp. 7423–7438, Jul. 2024.

[8] Ö. T. Demir and E. Björnson, "Wideband channel capacity maximization with beyond diagonal RIS reflection matrices," *IEEE Wireless Commun. Lett.*, vol. 13, no. 10, pp. 2687–2691, Oct. 2024.

[9] Q. Li et al., "Reconfigurable intelligent surfaces relying on non-diagonal phase shift matrices," *IEEE Trans. Veh. Technol.*, vol. 71, no. 6, pp. 6367–6383, Jun. 2022.

[10] Q. Li et al., "Coordinated reconfigurable intelligent surfaces: Non-diagonal group-connected design," *IEEE Trans. Veh. Technol.*, vol. 73, no. 7, pp. 10811–10816, Jul. 2024.

[11] T. D. Hua et al., "Cell-free massive mimo SWIPT with beyond diagonal reconfigurable intelligent surfaces," in *Proc. IEEE Wireless Commun. Netw. Conf. (WCNC)*, 2024, pp. 1–6.

[12] P. Del Hougne, "A physics-compliant diagonal representation for wireless channels parametrized by beyond-diagonal reconfigurable intelligent surfaces," *IEEE Trans. Wireless Commun.*, vol. 24, no. 7, pp. 5871–5884, Jul. 2025.

[13] J. Tapie et al., "Beyond-diagonal RIS prototype and performance evaluation," 2025, *arXiv:2505.13392*.

[14] D. Gürgünoğlu et al., "Power adaptation for vector parameter estimation according to Fisher information based optimality criteria," *Signal Process.*, vol. 192, Mar. 2022, Art. no. 108390.

[15] E. Björnson and Ö. T. Demir, "Capacity maximization for MIMO channels assisted by beyond-diagonal RIS," 2024, *arXiv:2411.18298*.

[16] I. Santamaria et al., "MIMO capacity maximization with beyond-diagonal RIS," in *Proc. IEEE 25th Int. Workshop Signal Process. Adv. Wireless Commun. (SPAWC)*, 2024, pp. 936–940.

[17] L. Dieci et al., "Takagi factorization of matrices depending on parameters and locating degeneracies of singular values," *SIAM J. Matrix Anal. Appl.*, vol. 43, no. 3, pp. 1148–1161, 2022.

[18] Q. Shi and M. Hong, "Penalty dual decomposition method for nonsmooth nonconvex optimization—Part I: Algorithms and convergence analysis," *IEEE Trans. Signal Process.*, vol. 68, pp. 4108–4122, 2020.

[19] J. R. Magnus and H. Neudecker, *Matrix Differential Calculus With Applications in Statistics and Econometrics*. New York, NY, USA: Wiley, 2019.

[20] M. K. Ercan et al., "RIS-aided NLOS monostatic multi-target sensing under angle-doppler coupling," *IEEE Trans. Veh. Technol.*, early access, Jul. 2, 2025, doi: 10.1109/TVT.2025.3585281.

Authorized licensed use limited to: ULAKBIM UASL - Bilkent University. Downloaded on December 11,2025 at 10:40:55 UTC from IEEE Xplore. Restrictions apply.